

# Forces between Hydrophilic Surfaces Adsorbed with Apolipoprotein AII Alpha Helices

S. Ramos, J. Campos-Terán,<sup>\*,†</sup> J. Mas-Oliva,<sup>‡</sup> Tommy Nylander,<sup>§</sup> and R. Castillo

*Instituto de Física, Universidad Nacional Autónoma de México, Post Office Box 20-364, D. F., México 01000, Departamento de Procesos y Tecnología, C. N. I., Universidad Autónoma Metropolitana-Cuajimalpa, Artificios 40, 6° Piso, D. F., México 01120, Instituto de Fisiología Celular, Universidad Nacional Autónoma de México, Post Office Box 70-243, D. F., México 04510, and Center for Chemistry and Chemical Engineering, Physical Chemistry 1, University of Lund, Post Office Box 124, SE-221 00 Lund, Sweden*

Received January 31, 2008. Revised Manuscript Received June 18, 2008

To provide better understanding of how a protein secondary structure affects protein–protein and protein–surface interactions, forces between amphiphilic  $\alpha$ -helical proteins (human apolipoprotein AII) adsorbed on a hydrophilic surface (mica) were measured using an interferometric surface force apparatus (SFA). Forces between surfaces with adsorbed layers of this protein are mainly composed of electrostatic double layer forces at large surface distances and of steric repulsive forces at small distances. We suggest that the amphiphilicity of the  $\alpha$ -helix structure facilitates the formation of protein multilayers next to the mica surfaces. We found that protein–surface interaction is stronger than protein–protein interaction, probably due to the high negative charge density of the mica surface and the high positive charge of the protein at our experimental conditions. Ellipsometry was used to follow the adsorption kinetics of this protein on hydrophilic silica, and we observed that the adsorption rate is not only controlled by diffusion, but rather by the protein–surface interaction. Our results for dimeric apolipoprotein AII are similar to those we have reported for the monomeric apolipoprotein CI, which has a similar secondary structure but a different peptide sequence and net charge. Therefore, the observed force curves seem to be a consequence of the particular features of the amphiphilic  $\alpha$ -helices.

## 1. Introduction

Forces that control the interaction between proteins, proteins and surfaces, surfaces with adsorbed proteins, as well as between proteins and polyelectrolytes, are the result of different contributions such as hydrophobic interaction, entropy gain due to counterion release, van der Waals force, and, to a large extent, electrostatic interactions, where the latter is governed by variables like pH and salt concentration. To understand how those different contributions modify the strength of protein interactions, one needs to start with proteins that have a relatively simple structure. Here, we have studied a small  $\alpha$ -helical protein human apolipoprotein AII (Apo AII) with an amphiphilic character, where a polar protein face is formed by charged amino acid residues clustered on one side of the  $\alpha$ -helix and a hydrophobic surface that is formed at the opposite face of the  $\alpha$ -helix composed of nonpolar residues. Thus, we expect that the orientation of this protein on surfaces is dependent on the hydrophobic/hydrophilic character of the surface, which makes it possible to form specifically oriented protein layers where the exposure of hydrophobic moieties to the aqueous solution is minimized.

Apo AII is the second major apolipoprotein (Apo) of high density lipoproteins (HDL) and it is synthesized in the liver.<sup>1</sup> This protein has been suggested as a modulator of reverse cholesterol transport rather than a strong determinant of lipid metabolism.<sup>2</sup> Apo AII is formed by two identical polypeptide

chains connected by a disulfide bridge at position 6, where each chain corresponds to 77 amino acid residues in length and a molecular mass of 8.708 kDa.<sup>3,4</sup> This protein has been extensively studied by our group. Predictive and circular dichroism studies,<sup>5,6</sup> as well as high resolution crystal structure studies,<sup>7</sup> have shown that each chain of the Apo AII presents two  $\alpha$ -helix motifs (peptides encompassing 7–27 and 32–67) as its main secondary structure, see Figure 1. These  $\alpha$ -helices present an important hydrophobic moment,<sup>6</sup> are approximately 31.5 and 54 Å in length, and they are connected by a short peptide chain as a loose hinge.<sup>6</sup> Correlation between protein stability to thermal denaturation and secondary structure content has also been investigated.<sup>6</sup> When these proteins are in contact with a polar/nonpolar media, they will anchor the hydrophilic and hydrophobic regions in the polar and in the nonpolar media, respectively. Thus, a hydrophobic/hydrophilic interface tends to induce a specific orientation on the adsorbed proteins. As mentioned, Apo AII is associated with lipoprotein particles that are modeled<sup>8</sup> as spheres with a shell of a phospholipid monolayer with the polar head groups oriented toward the aqueous phase, and the core consists of triglycerides and cholesterol esters (hydrophobic region). In these models, Apos are usually oriented parallel to the surface of the lipoprotein particles.<sup>6</sup> One way to characterize the interaction between  $\alpha$ -helices (Apos) and the lipoprotein surface is to deposit them

(3) Brewer, H. B.; Ronan, R.; Meng, M.; Bishop, C. *Methods Enzymol.* **1986**, *128*, 223.

(4) Brewer, H. B.; Lux, S. E.; Ronan, R.; John, K. M. *Proc. Natl. Acad. Sci. U.S.A.* **1972**, *69*, 04.

(5) Bolaños-García, V. M.; Soriano-García, M.; Mas-Oliva, J. *Mol. Cell. Biochem.* **1997**, *175*, 1.

(6) Bolaños-García, V. M.; Mas-Oliva, J.; Ramos, S.; Castillo, R. *J. Phys. Chem. B* **2001**, *105*, 5757.

(7) Kumar, M. S.; Carson, M.; Hussain, M. M.; Murthy, H. M. *Biochemistry* **2002**, *41*, 11681.

(8) Borhani, D. W.; Rogers, D. P.; Engler, J. A.; Brouillette, C. G. *Proc. Natl. Acad. Sci. U.S.A.* **1997**, *94*, 2291.

\* To whom correspondence should be addressed. E-mail: jcampos@correo.cua.uam.mx.

<sup>†</sup> Departamento de Procesos y Tecnología, C. N. I.

<sup>‡</sup> Instituto de Fisiología Celular, UNAM.

<sup>§</sup> University of Lund.

(1) Eggerman, T. L.; Howg, J. M.; Meng, M. S.; Tombragel, A.; Baojanovski, D.; Brewer, H. B. *J. Lipid Res.* **1991**, *32*, 821.

(2) Tailleux, A.; Duriez, P.; Fruchart, J. C.; Clavey, V. *Atherosclerosis* **2002**, *164*, 1.

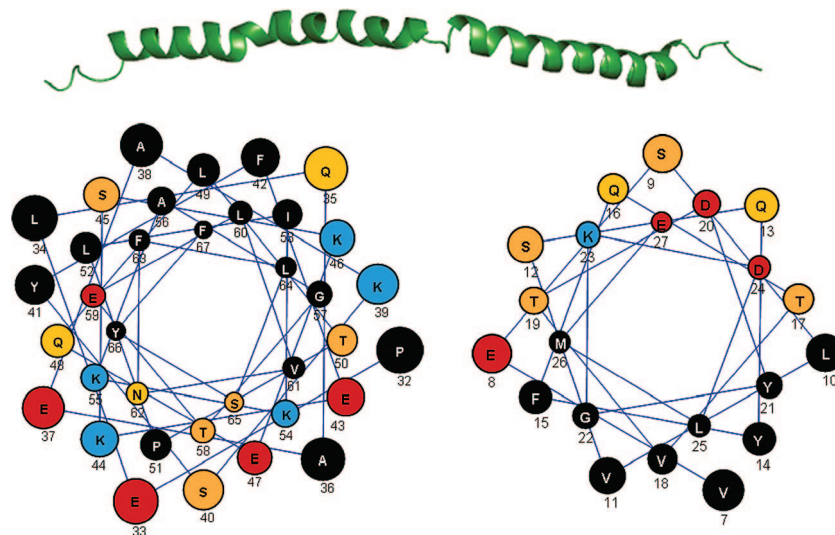


**Figure 1.** Secondary structure scheme and helical wheel projections for the  $\alpha$ -helices of Apo AII. These  $\alpha$ -helices are approximately 54 and 31.5 Å in length and they are connected by a short peptide chain as a loose hinge.<sup>6</sup> Hydrophobic, polar without charge, negative-charged, and positive-charged peptides are represented by black, yellow, red, and blue circles, respectively.

on a surface that mimics the lipoprotein surface. This allows us to measure directly the strength of the interaction between proteins and surfaces, as well as between protein covered surfaces. We have previously investigated the interaction of  $\alpha$ -helices at the air/water interface by studying Apo AII Langmuir monolayer during compression.<sup>6,9</sup> Two first-order phase transitions were found, where one of the transitions occurs at high lateral pressure,  $\Pi \sim 30\text{--}35 \text{ mNm}^{-1}$  and  $A \sim 1000\text{--}2500 \text{ Å}^2/\text{molecule}$ . This transition involves two phases, a liquid phase (L) and a condensed phase (LC), that correspond to a conformational change. In the liquid phase, the protein configurations are restricted to a horizontal orientation at the interface due to the amphiphilic character of this protein. As the surface area is decreased on isothermal compression, two of the four  $\alpha$ -helix segments of the protein molecule are expelled from the interface. Direct evidence of this conformational change, as well as of the  $\alpha$ -helix structure of Apo AII, have been shown using grazing incidence X-ray diffraction and atomic force microscopy (AFM) of Langmuir–Blodgett (LB) films of transferred protein monolayers.<sup>9</sup> Experiments using more complex interfaces that are closer to the lipoprotein surface have also been used; for example, we studied the adsorption of Apo AII on *rac*-1,2-dipalmitoyl-*sn*-glycero-3-phosphocholine (DPPC) monolayer.<sup>10</sup> The results indicate that apolipoproteins can penetrate the DPPC monolayer to form part of it at the air/water interface; also, phase transitions of this penetrated monolayer have been studied.<sup>10</sup>

When two surfaces with adsorbed layers of proteins are brought together, the resulting force versus distance curve will depend on the kind of surface and the solution where the protein is immersed, as well as on charge, shape, and conformation of the protein. The surface force apparatus (SFA) offers the possibility of measuring long-range and contact forces between two mica surfaces covered with adsorbed protein, as well as, of measuring the adsorbed layer thickness and its compressibility. The latter parameter can give information about the conformational structure and size of the adsorbed protein. The comparison between theoretical and experimental force curves is not straightforward, because the measured force is the sum of different contributions,

which are interrelated and therefore not easy to separate. The electrostatic-double layer force and the van der Waals force are considered the most important contributions. However, an absolute determination of the magnitude of each of these forces is complex, due to factors as protein and surface charge density, protein concentration, solution ionic strength, contribution from steric interactions at short distances, and so on. In addition, the location of the plane of charge and the dielectric properties of the adsorbed protein layer usually cannot be determined unambiguously. Nevertheless, the results from SFA studies of the interaction between layers of globular proteins, like insulin and lysozyme, and of proteins with disordered structures have increased our knowledge on the adsorbed layer structure.<sup>11</sup> This also includes our previous SFA study of a protein formed mainly by an  $\alpha$ -helix structure, Apo CI.<sup>12</sup>

Apo CI and Apo AII are members of a family of proteins that are membrane active proteins, which apparently give lipoproteins directionality and the ability to interact with receptors at the surface of cells. Also, they can dissociate and transfer among lipoproteins. A detailed knowledge of the interaction of these apolipoproteins with surfaces could be of help to understand their biological function. The aim of this paper is to understand the adsorption process of amphiphilic Apo AII on hydrophilic model surfaces (silica and mica), as well as, to study the nature of protein–surface and protein–protein interactions. For this purpose, we have used ellipsometry to follow the adsorption kinetics on a hydrophilic silica surface, and to provide us with a deeper insight of the interactions, force measurements as a function of surface separation between two apolipoprotein-covered mica surfaces were carried out.

## 2. Experimental Section

**Reagents.** Lyophilized human apolipoprotein AII (Apo AII) (>98%, PerImmune Incorporation, U.S.A., and >96% Sigma-Aldrich, Inc., U.S.A.) was used. Circular dichroism (CD) was used to verify protein structural integrity in the solutions used for the experiments. Water was ultrapure Milli-Q water (Nanopure-UV, U.S.A.; 18.3 M $\Omega$ ), filtered through a 0.22  $\mu\text{m}$  membrane filter prior

(9) Ruiz-García, J.; Moreno, A.; Brezesinski, G.; Möhwald, H.; Mas-Oliva, J.; Castillo, R. *J. Phys. Chem. B* **2003**, *107*, 11117.

(10) Xicohtencatl-Cortés, J.; Mas-Oliva, J.; Castillo, R. *J. Phys. Chem. B* **2004**, *108*, 7307.

(11) Claesson, P. M.; Blomberg, E.; Fröberg, J. C.; Nylander, T.; Arnebrant, T. *Adv. Colloid Interface Sci.* **1995**, *57*, 161.

(12) Campos-Terán, J.; Mas-Oliva, J.; Castillo, R. *J. Phys. Chem. B* **2004**, *108*, 20442.

to be injected into the SFA. A buffer solution of acetic acid (>99.99%, Sigma-Aldrich, MO) and sodium acetate (>99.995%, Sigma-Aldrich, MO) was used to obtain a pH = 4. The ionic strength of the solution, taking into account all ionic species, that is,  $1 \times 10^{-4}$  M from  $H^+$  and  $7.12 \times 10^{-5}$  M from  $Na^+$ , corresponds to  $1.71 \times 10^{-4}$  M of a 1:1 electrolyte.

**Surface Force Measurements.** An interferometric SFA was used to measure the interaction between adsorbed layers of Apo AII on hydrophilic mica. Instruments and procedures have been described by Israelachvili,<sup>13</sup> and the particular version of the apparatus that we used in this study (Mark IV) has been described by Parker et al.<sup>14</sup> Force is measured between two curved mica surfaces (mean radius of curvature,  $R$ ,  $\sim 1$ –2 cm) in a crossed cylinder configuration obtained by two mica sheets (typically  $1 \text{ cm}^2$  of area with  $2$ – $5 \text{ }\mu\text{m}$  constant thickness), supported on half-cylindrical silica disks; the first one is mounted on a double cantilever spring (spring constant,  $k$ ,  $\sim 105 \text{ N/m}$ ) and the second one on a piezoelectric crystal. The separation between the two surfaces,  $d$ , is controlled by the piezoelectric crystal and the absolute distance is measured interferometrically using fringes of equal chromatic order (FECO) with an accuracy of  $2 \text{ \AA}$ . The magnitude of the force,  $F$ , as a function of the surface separation, normalized with respect to the mean radius curvature, can be determined from the spring deflection measured down to about  $10^{-7} \text{ N}$ . Micrometer thick and monomolecular smooth sheets were cleaved from green muscovite mica (S&J Trading Inc., NY) and cut into  $1 \times 1 \text{ cm}$  pieces. A silver (>99.99%, Aldrich Chem. MO) layer of about  $520 \text{ \AA}$  thick was deposited through evaporation on one side of each sheet. The mica pieces were glued (epoxy resin EPON 1004F, Young modulus  $\sim 2 \times 10^{10} \text{ dyn cm}^{-2}$ , Shell Chemical Co.), with the silver side down, onto optically polished half-cylindrical silica disks that were finally mounted on the SFA to produce an optical interferometer.<sup>14</sup> Before each experiment, the instrument equipped with a volume chamber of  $40 \text{ mL}$  was dismantled and all the inner parts were rinsed with water, anhydrous ethanol (Spectroscopy grade, Merck, Darmstadt, Germany), and finally blown dried with ultrapure nitrogen before assembling them again. The assembly of the instrument and surface preparation were performed in a clean room under essentially dust-free conditions. All force measurements were carried out at  $21 \text{ }^\circ\text{C}$ .

**Surface Measurements of Apo AII on Hydrophilic Surfaces (Mica).** Experiments start measuring the FECO for the mica–mica contact position,  $d = 0$ , in nitrogen. Both forms of fringes and the measured surface adhesion determined if the mica surfaces are free from contaminants. Then, the SFA is filled with acetic acid–sodium acetate buffer solution (pH = 4, with  $1.712 \times 10^{-4} \text{ M}$  1:1 electrolyte). After an equilibration time of usually  $1 \text{ h}$ , the contact position is checked up and a force curve is recorded to verify if the surfaces are clean and the measured force curve is as expected one from DLVO theory. A nonfiltered aliquot of Apo AII stock solution is then added into the SFA chamber and force curves are measured after different adsorption times. Here we note that the surfaces were allowed to equilibrate for about  $1 \text{ h}$  at a surface separation of  $2 \text{ nm}$  before recording the first force curve. In some experiments, the amount of protein concentration was sequentially increased. In other experiments, after having reached equilibrium with respect to protein adsorption, we removed the solution from the chamber, just leaving a small drop of the solution between the mica surfaces. Then, a fresh protein-free buffer solution was added. All our forces curves correspond to “first approach,” except those explicitly mentioned in the manuscript. The rate of approach was around  $10 \text{ \AA/s}$ , which allowed us to measure all the experimental points in the force curves close to equilibrium.

**Ellipsometry.** An automated thin-film null ellipsometer (Rudolph Research model 43603–200E, U.S.A.) was used as described by Tiberg and Landgren<sup>15</sup> to measure, in situ, the amount and thickness of adsorbed protein layers at silica surfaces. The silicon surfaces

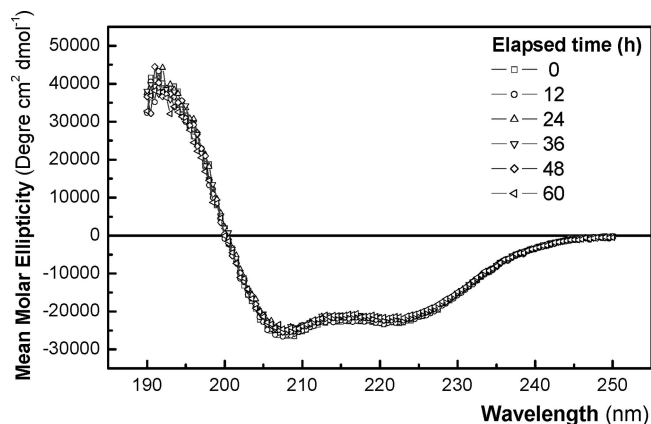


**Figure 2.** Protein integrity as a function of time. Far-ultraviolet CD spectra for Apo AII dispersed in acetic acid–sodium acetate buffer solution (pH = 4.0,  $20 \text{ }^\circ\text{C}$ ) as a function of elapsed time from solution preparation.

were thermally oxidized in an oxygen atmosphere at  $920 \text{ }^\circ\text{C}$  for  $\sim 1 \text{ h}$ , followed by annealing and cooling in an argon flow. This procedure yields a  $\text{SiO}_2$  layer of  $\sim 30 \text{ nm}$  thickness. The oxidized wafers were cut into slides with a width of  $12.5 \text{ mm}$  and cleaned in a mixture of (1)  $\text{NH}_4\text{OH}-\text{H}_2\text{O}_2$  and (2)  $\text{HCl}-\text{H}_2\text{O}_2$ , as described earlier.<sup>15</sup> Finally, the cleaned oxidized surfaces were stored in ethanol. Prior to the start of the ellipsometric experiments, the surfaces were dried under vacuum ( $0.001 \text{ mbar}$ ) and then treated in a plasma cleaner (Harrick Scientific Corp., model PDC-3XG, U.S.A.) for  $5 \text{ min}$ . The optical properties of silica surfaces, that is, refractive index of the silicon and the oxidized layer, as well as, the oxidized layer thickness, were characterized at the beginning of each experiment by measuring the ellipsometric angles,  $\Psi$  and  $\Delta$ , in two different ambient media: in air and in an acetic acid–sodium acetate buffer solution (pH=4), as described earlier.<sup>16</sup> All measurements were performed with a light-source wavelength of  $4015 \text{ \AA}$  and with an angle of incidence of  $\sim 68^\circ$ . All experiments were carried out in a  $5 \text{ mL}$  cuvette that was thermostatted to  $25.0 \pm 0.1 \text{ }^\circ\text{C}$  and agitated with a magnetic stirrer at  $\sim 300 \text{ rpm}$ . The recorded ellipsometric angles were evaluated using a four-layer optical model, assuming isotropic media and planar interfaces. The mean refractive index,  $n_f$ , and the ellipsometric thickness,  $d_f$ , of the adsorbed layer were calculated numerically as described elsewhere.<sup>17,18</sup> The adsorbed amount,  $\Gamma$ , was calculated from  $n_f$  and  $d_f$  using the following formula

$$\Gamma = \frac{(n_f - n_0)d_f}{dn/dc}$$

where  $n_0$  is the refractive index of the bulk solution and  $dn/dc$  is the refractive index increment as a function of the bulk concentration. For Apo AII solutions a value of  $dn/dc = 0.154 \text{ cm}^3/\text{g}$  was used, as it is common with other proteins and peptides.<sup>19,20</sup>

### 3. Results and Discussion

**Structural Stability and Charge of Apo AII.** Far-ultraviolet CD spectra for dispersed Apo AII in acetic acid–sodium acetate buffer solution (pH = 4.0,  $20 \text{ }^\circ\text{C}$ ), as a function of time from the solution preparation, are presented in Figure 2. In all the cases, spectra present two minimum. The first one occurs around  $208 \text{ nm}$ , which corresponds to both  $\alpha$ -helix  $\pi-\pi^*$  and to random coil  $\pi-\pi^*$  transitions. The second one is at about  $222 \text{ nm}$ , which corresponds to an  $\alpha$ -helix  $n-\pi$  transition. These values are

(16) Landgren, M.; Jönsson, B. *J. Phys. Chem.* **1993**, *97*, 1656.

(17) Jenkins, T. E. *J. Phys. D: Appl. Phys.* **1999**, *32*, R45.

(18) Azzam, R. M. A.; Bashara, N. M., *Ellipsometry and Polarized Light*; North-Holland Publishing Co.: Amsterdam, 1977.

(19) Malmsten, M.; Bergenstahl, B.; Masquelier, M.; Pålsson, M.; Peterson, C. *J. Colloid Interface Sci.* **1995**, *172*, 485.

(20) Ringstad, L.; Schmidtchen, A.; Malmsten, M. *Langmuir* **2006**, *22*, 5042.

(13) Israelachvili, J. N.; Adams, G. E. *J. Chem. Soc., Faraday Trans. 1* **1978**, *74*, 975.

(14) Parker, J. L.; Christenson, H. K.; Ninham, B. W. *Rev. Sci. Instrum.* **1989**, *60*, 3135.

(15) Tiberg, F.; Landgren, M. *Langmuir* **1993**, *9*, 927.



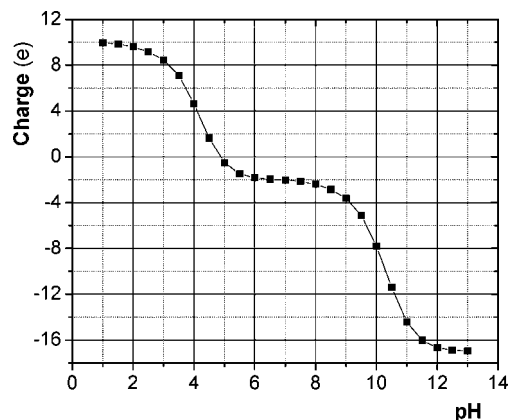


**Figure 3.** Apo AII charge vs pH calculated from its amino acid composition for one chain.<sup>22</sup>

considered typical for  $\alpha$ -helix motives.<sup>21,22</sup> Spectra show that the secondary structure of Apo AII is well preserved in the buffer solution for more than 60 hours. This verifies that the structure of the protein does not change during the force measurements, which usually takes 2 or 3 days. Similar results were found for both protein batches.

Figure 3 shows the charge,  $Q$ , of Apo AII as a function of pH, calculated from the amino acid sequence, assuming that there are no electrostatic interactions that could perturb ionization.<sup>23</sup> The obtained isoelectric point corresponds to  $\text{pH} = 4.85$ . Our adsorption studies and force measurements were conducted close to  $\text{pH} = 4$ , where the net charge of Apo AII is about  $+10 e$  ( $+5 e$  per chain).

**Adsorption of Apo AII on Silica Surfaces.** Ellipsometry measurements were carried out to follow Apo AII adsorption kinetics on silica surfaces for a short time scale. This technique offers a convenient way to screen the interfacial behavior of Apo AII on surfaces. Although for technical reasons we are using different surfaces to those used in the SFA experiments, both silica and mica are negatively charged. In addition, in several studies we have observed that protein adsorption behaves quite similar on these two surfaces, that is, lipase,<sup>24</sup>  $\beta$ -casein,<sup>25,26</sup> lysozyme,<sup>27,28</sup> and insulin.<sup>29,30</sup> The results from these adsorption studies provide complementary information to surface force measurements. The data for different adsorption conditions for Apo AII are summarized in Table 1, and typical adsorption curves showing both adsorbed amount and layer thickness versus time are given in Figure 4. Due to the low protein concentration, the adsorption kinetics is slow and a steady state is reached only after several hours. Figure 4a shows the adsorption curve at pH 4, and Figure 4b at pH 4.5. We observed that the adsorption kinetics is different although the protein concentration is the same. Thus, we can conclude that the adsorption rate is not only

controlled by diffusion, but rather by the protein–surface interaction. It is apparent from the observed pH dependence that the interaction is of electrostatic nature, because a less amount of adsorbed protein is obtained closer to its isoelectric point. However, electrostatics does not only govern the protein surface interaction, where increasing opposite charges between surface and protein are expected to increase the protein adsorbed amount. In addition, the surface charge on silica is also dependent on the ionic strength (and adsorbing species as will be discussed further below), and an increase in ionic strength will lead to an increase in deprotonated OH groups at the silica surface.<sup>31</sup> Consequently, this will lead to an increase in the adsorption of cationic species. This is obvious from the data shown in Figure 4c, where we show the corresponding data at high ionic strength and pH 4. In this case, we see a significant increase in the total adsorbed amount of protein compared to the data in Figure 4a. Here, in addition to an increment in surface charge, adsorption is enhanced because when the ionic strength increases, a screening of the electrostatic repulsion between charged species is produced, which allows the formation of a more densely packed layer. We also note that, no matter the pH, a sequential increase in the protein concentration from 0.002 mg/mL to 0.004 mg/mL leads to an augment in the total adsorbed amount of protein. These adsorbed amounts corresponds to a quantity less than or equal to that expected for a protein monolayer on a surface.

**Measurements of Surface Force Interaction.** The force curve versus surface separation between mica surfaces in protein-free acetic acid–sodium acetate buffer solution ( $\text{pH} = 4$ ) is shown in Figure 5. This force curve is consistent with the force predicted by DLVO theory and it shows a long-ranged repulsive electrostatic double-layer force, as the mica surfaces are negatively charged due to the release of potassium ions into the solution. We fitted the curve with a double layer force calculated with the algorithm described by Chan et al.<sup>32</sup> using a constant charge boundary condition. It gives a Debye length of  $232.8 \text{ \AA}$  and a surface potential ( $\Psi_0^\infty$ ) of 90 mV. This experimental decay length correlates well with the theoretical one expected for our 1:1 electrolyte solution at  $1.71 \times 10^{-4} \text{ M}$ , which is of  $232.4 \text{ \AA}$ .<sup>33</sup> When the surfaces are brought close together, this force is overcome by an attractive van der Waals force at a surface separation of  $20 \text{ \AA}$ , pulling the mica surfaces into a strong adhesive contact ( $d \sim 3 \text{ \AA}$ ). The van der Waals force was calculated using a Hamaker constant of  $A = 2.2 \times 10^{-20} \text{ J}$  for mica interacting across water.<sup>33</sup>

**Protein Adsorption Affects the Short-Range Interaction.** The measured force curve versus surface separation between mica surfaces, interacting across an acetic acid–sodium acetate buffer solution ( $\text{pH} = 4$ ), containing 0.002 mg/mL of Apo AII is also presented in Figure 5. When Apo AII was injected into the SFA chamber, large changes were found with respect to the force found in the protein-free buffer solution. Although the force curves recorded at 3.5, 27 and 72 h after protein addition turned out to be very similar, we can observe that the interaction between the surfaces changes during the protein adsorption process. In all cases the force is negligible when the surfaces are separated for more than  $\sim 700 \text{ \AA}$ . When the surfaces are brought together a long-range repulsive force is observed until it is overcome by an attractive force, which brings the surfaces from a surface separation of about  $150\text{--}200 \text{ \AA}$  into a closer contact

(21) Manavalan, P.; Johnson, W. C., Jr. *Nature* **1983**, *305*, 831.

(22) Greenfield, N. J. *Anal. Biochem.* **1996**, *235*, 1.

(23) Program by L. Toldo. Modified by B. Kindler. Available at EMBL WWW Gateway to Isoelectric Point Service <http://www.embl-heidelberg.de/cgi/pi-wrapper.pl>.

(24) Campos, J.; Eskilsson, K.; Nylander, T.; Svendsen, A. *Colloids Surf., B* **2002**, *26*, 172.

(25) Nylander, T.; Wahlgren, M. N. *Langmuir* **1997**, *13*, 6219.

(26) Kull, T.; Nylander, T.; Tiberg, F.; Wahlgren, M. N. *Langmuir* **1997**, *13*, 5141.

(27) Blomberg, E.; Claesson, P. M.; Fröberg, J. C.; Tilton, R. D. *Langmuir*, *10*, 2325.

(28) Wahlgren, M.; Arnebrant, T.; Lundstrom, I. *J. Colloid Interface Sci.* **1995**, *175*, 506.

(29) Nylander, T.; Kékicheff, P.; Ninham, B. W. *J. Colloid Interface Sci.* **1994**, *164*, 136.

(30) Nilsson, P.; Nylander, T.; Havelund, S. *J. Colloid Interface Sci.* **1991**, *144*, 145.

(31) Shamoshina, Y.; Nylander, T.; Shubin, V.; Bauer, R.; Eskilsson, K. *Langmuir* **2005**, *21*, 5872.

(32) Chan, D. Y. C.; Pashley, R. M.; White, L. R. *J. Colloid Interface Sci.* **1980**, *77*, 283.

(33) Israelachvili, J. N. *Intermolecular and Surface Forces*, 2nd ed.; Academic Press: New York, 1992.

**Table 1. Ellipsometry Results for Adsorbed Apo AII on Silica**

Apo AII concentration (mg/mL)	pH	time to reach adsorption plateau(s) <sup>a</sup>	adsorbed amount (mg/m <sup>2</sup> )	layer thickness (Å)
0.002	4	~20000	0.2	93
0.004	4	~35000	0.57	115
0.002	4.5	~2000	0.1	not accessible at this adsorbed amount
0.004	4.5	no observed plateau	~0.43 @ $t = 6 \times 10^4$ s	40
0.002	4 + 150 mM NaCl	~11000	1	141
0.004	4 + 150 mM NaCl	~18000	1.8	185

<sup>a</sup> Time measured since the last aliquot addition, not total experimental time.

(attractive jump). The surface separation, where the attractive force drives the surfaces close together, decreases with adsorption time as shown in Table 2. After 3.5 h, the attractive force brings the surfaces from a surface separation of  $d = 197$  Å to  $d = 56$  Å. We then observe a weak repulsive force, which can be overcome by applying additional force until we reach a repulsive hard wall at about 11 Å. After 27 h, this weak repulsive force has been significantly reduced and it is not detectable after 72 h. In all force curves measured at 0.002 mg/mL in Apo AII, the hard wall contact is at  $d = 11$  Å and the force needed to pull the surfaces apart from this position always corresponds to an adhesion force of ~40 mN/m (data is not shown). If the adhesion is measured just before the hard wall position a value of ~35 mN/m was measured. Here, we note that the force curves are the same on compression and on separation if the surfaces are not brought closer than the inward jump.

Fitting DLVO theory to the experimental force curves gives a mean decay length around 232 Å and a decrease in the apparent interfacial potential to approximately  $\Psi_0^\infty = 40$  mV, compared to  $\Psi_0^\infty = 90$  mV for the pure buffer solution. For these calculations, we assumed that the plane of charge and the origin of the van der Waals force are located at the position of the hard wall repulsion, that is,  $d \sim 11$  Å. If the fitting was done using the position where the protein layers come into first contact, then a value of 35 mV in the apparent interfacial potential was found. The Hamaker constant used here was  $0.5 \times 10^{-20}$  J, which corresponds to the value for a hydrocarbon layer interacting across water, which is a common value used for protein layers.<sup>11</sup> This is a reasonable first guess because the dielectric function for a protein is higher than for hydrocarbon, but this is partly compensated by the rather high water content in the layer. In addition, this value corresponds to a lower value similar to that of the main constituents of the hydrophobic side of Apo AII. Both boundary conditions were considered, i.e., constant surface charge and constant surface potential. In most cases neither surface charge nor surface potential remain constant as the solution conditions change. This is because ionizable surface sites are rarely fully dissociated but are partially neutralized by the binding of specific ions from the solution. In general, the interaction potential will lie between these two limits. Lund et al.<sup>34</sup> have shown the importance of an enhanced protein adsorption due to charge regulation, that is, the effective protein net charge changes due to the proximity of a charged surface. The effect can be understood in terms of the protein capacitance  $C = -(1/\ln 10)(\partial Q/\partial \text{pH})$ ,<sup>34</sup> a property that quantifies the protein ability for charge fluctuation. As it can be observed in Figure 2, at pH = 4, this effect could play an important role and, as expected, the experimentally determined force curves lie between both boundary conditions, almost certainly due to Apo AII charge regulation. Also, it should be pointed out that we have performed the force curve fittings assuming a monovalent electrolyte

solution. For the case of highly charged proteins, it has been observed<sup>35,36</sup> that corrections are needed to take into account the high charge in the total number of charges in the double layer system. Nevertheless, in our case, we found that these corrections are small because our protein concentration is 3 orders of magnitude less than that of the electrolyte solution. Thus, the measured decay found in our force curves corresponds to the same order as the theoretically expected value of 232.4 Å for our  $1.712 \times 10^{-4}$  M 1:1 electrolyte solution.

**Short Range Forces Probe the Orientation of the Adsorbed Protein.** The average distance where the attractive force appears,  $d \sim 150$  Å, is close to double that of the maximum length of Apo AII (~85 Å), which suggests that the entire protein is oriented perpendicular to the surface or that individual protein segments, that is,  $\alpha$ -helices, protrude from the surfaces. These protein segments could take part in bridging between the two surfaces and, thus, be responsible for the attractive force. This kind of attractive force has been observed before in adsorbed surfaces with  $\beta$ -casein,<sup>25</sup> which is a flexible nonglobular protein, as well as in protein A<sup>37</sup> and Apo CI.<sup>12</sup> Studies of Apo AII monolayers have shown that it is possible to form a layer with protruding segments at an interface.<sup>6,9</sup> Our ellipsometry data presented in Figure 4a also indicate a layer thickness of about 100 Å, although thickness determination using ellipsometry is somewhat uncertain for low adsorbed amounts. The fact that, at short adsorption time, we observe a weak repulsive force, suggests a more extended conformation of the adsorbed proteins. Such protruding segments could be compressed, bearing in mind the relative flexibility of the polypeptide chains connecting the  $\alpha$ -helices. Given enough time for adsorption, the protein molecule preferentially will be oriented parallel to the surface and, hence, this repulsive force disappears. The driving force for protein reorientation is to avoid the exposure of hydrophobic segments to the aqueous environment, as well as to promote the electrostatic attractive interactions between the protein and the surface. We also note that the attractive interaction is reduced with time, which implies a higher protein surface coverage confined in a thin layer. This thin protein layer was found experimentally since we observed a surface separation of just 11 Å at the hard wall position. Also, this final layer thickness value is 5–6 Å on each surface, which is similar to the estimated value for  $\alpha$ -helices diameter. Previously, it has been shown that structural changes on adsorption are not enough to disturb the  $\alpha$ -helix structure.<sup>38</sup> It is noteworthy that we observed quite similar force curves in Apo CI,<sup>12</sup> which also has a similar secondary structure. However, Apo CI has a different peptide sequence, a different net charge, and it is only monomeric. Therefore, the observed force curves seem to be a consequence of the particular features of the amphiphilic  $\alpha$ -helices.

(35) Kekicheff, P.; Ninham, B. W. *Europhys. Lett.* **1990**, *12*, 471.

(36) Nylander, T.; Kekicheff, P.; Ninham, B. W. *J. Colloid Interface Sci.* **1994**, *164*, 136.

(37) Ohnishi, S.; Murata, M.; Hato, M. *Biophys. J.* **1998**, *74*, 455.

(38) Burkett, S. L.; Read, M. J. *Langmuir* **2001**, *17*, 5059.

(34) Lund, M.; Åkesson, T.; Jönsson, B. *Langmuir* **2005**, *21*, 8385.

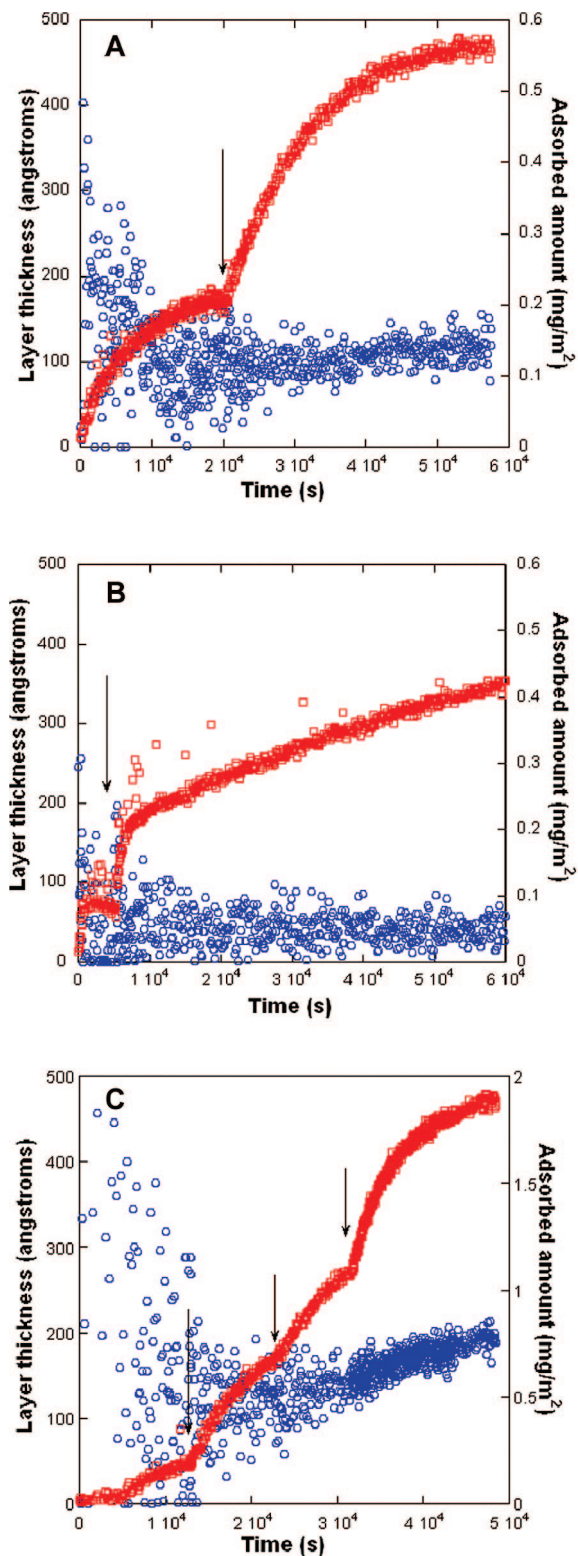


**Figure 4.** Adsorbed amount (red open squares) and adsorbed layer thickness (blue open circles) as a function of time for Apo AII on silica measured by ellipsometry, at different pH: (A) pH = 4.0, (B) pH = 4.5, and (C) pH = 4.0 in a 150 mM NaCl electrolyte solution. In (A) and in (B), the arrow indicates the addition of protein to increase the total protein concentration from 0.002 to 0.004 mg/mL. In (C), arrows indicate protein increase from 0.0005 to 0.0014, from 0.0014 to 0.002, and from 0.002 to 0.004 mg/mL.

**Effect of Protein Concentration on the Adsorbed Layer.**

Figure 6 shows the force curves measured 5 and 24 h after injection of 0.004 mg/mL of Apo AII. The force curves are similar to the

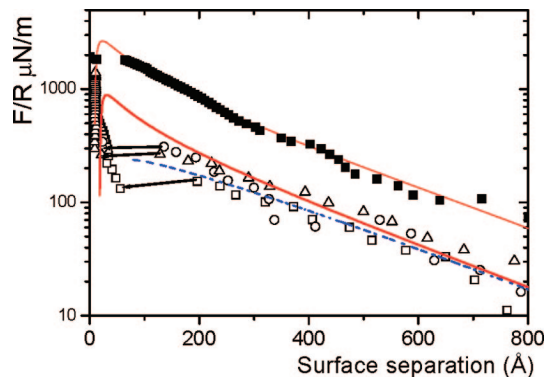


**Figure 5.** Force normalized by the radius of curvature,  $F/R$ , as a function of surface separation between mica surfaces adsorbed with Apo AII after 3.5 ( $\square$ ), 27 ( $\circ$ ), and 72 ( $\Delta$ ) h of protein adsorption time from a protein solution of 0.002 mg/mL. It is also included the force curve ( $\blacksquare$ ) for the buffer protein-free solution. Lines indicate DLVO fitting with constant surface charge and dashed lines with constant surface potential. Details of the fittings can be found in the text. Arrows indicate attractive jumps.

ones described in Figure 5, and here we will only discuss the main differences. One of these differences is that the hard wall is located at  $d \approx 60 \text{ \AA}$ . We also observed that the attractive force observed after 5 h (surfaces jump into contact from  $d \approx 210 \text{ \AA}$ ) disappears after 24 h. Furthermore, the adhesive pull-off force is reduced to 15 mN/m compared to 40 mN/m for the lower concentration. These observations are a clear indication of an increase in protein adsorption at the surfaces. This is also observed with ellipsometry for a similar increase of protein concentration (Figure 4a). If we consider that the protein molecules are mainly adsorbed in a side-on orientation, the observed thickness of 30  $\text{\AA}$  on each surface corresponds to 2–3 not well-ordered adsorbed layers of Apo AII. The formation of multilayers will be discussed further below, but this is likely to be a self-assembly process where proteins want to avoid their hydrophobic moieties to be exposed to the water solution.

**Sequential Addition Builds up Protein Multilayers.**

Experiments conducted at higher concentrations suggest the build up of more than one layer on each surface. This was further explored by sequentially increasing the protein concentration. In fact the results from ellipsometry measurements presented in Figure 4 shows that sequential addition of protein (at least at high ionic strength) leads to an increase in the adsorbed amount of protein, as well as the protein layer thickness. To further investigate this self-assembly process, we also conducted SFA experiments with a sequential increase of protein concentration; Figure 7 shows the results. First, we note that the DLVO theory considering a 1:1 electrolyte fits the data with an average decay length of 232  $\text{\AA}$  and apparent surfaces potential  $\sim 39$  and  $\sim 37$  mV, when the protein concentrations were 0.002 and 0.004 mg/mL, respectively. This long-range repulsive interaction shows that protein adsorption do not lead to charge neutralization of the mica surface charge as it was found for Apo CI.<sup>12</sup> This is most likely due to the structural difference between both proteins, where the Apo CI monomer can more efficiently arrange so that it better match the surface charge compare to the Apo AII dimer. However, since the apparent surface potential has a small change when the protein concentration is increased from 0.002 to 0.004 mg/mL, a charge regulation mechanism involving small ions during the adsorption of the proteins cannot be discarded. This mechanism

(39) Kekicheff, P.; Ducker, W. A.; Ninham, B. W.; Pileni, M. P. *Langmuir* **1990**, *6*, 1704.

(40) Dathe, M.; Wieprecht, T. *Biochim. Biophys. Acta* **1999**, *1462*, 71.



**Table 2. Surface Force Measurement Results for Adsorbed Apo AII on Mica (pH = 4)**

figure	Apo AII concentration (mg/mL)	adsorption time (h)	range of attractive interaction; initial–final distance (Å)	distance of repulsive steric wall (Å)	surface potential from DLVO fitting <sup>32</sup> ( $\Psi_0^\infty$ , mV)
5	0		20–3	0	90
5	0.002	3.5	197–56	11	40
		27	135–24	11	40
		72	129–22	11	40
6	0.004	5	210–115	60	45
		24		60	45
7	0.002	5	81–13	13	39
		6.5	142–38	38	37
		8		38	37
		25		49	37
		29		58	37
8 (rinsing)	0.004	1.5		26	53
		18	120–18	11	53

has been observed to occur in the surface adsorption of other proteins<sup>11</sup> and, as we mentioned before, usually the interaction force curve measured lies between the two boundary conditions, that is, constant surface charge and constant surface potential. The force curve recorded  $\sim 5$  h after adding 0.002 mg/mL in Apo AII is as expected similar to those shown in Figure 5 after similar time. The force curve 1.5 h (6.5 h of the first protein injection) after the second Apo AII addition (to 0.004 mg/mL) is quite similar to the one measured before but here, the attractive force leads to inward jump from  $d \approx 142$  Å, to a hard wall at  $d \approx 38$  Å. As discussed above, the attractive force disappears if enough time is given to the protein to adsorb, but here the surface separation value for the hard wall contact increases with protein adsorption time:  $d \approx 38$  Å after 8 h of protein adsorption,  $d \approx 49$  Å after 25 hours, and  $d \approx 58$  Å after 29 h, all of them after the addition of the first protein aliquot. Each curve shown in Figure 7 represents an increase in hard-wall separation of  $\sim 10$  Å or approximately 5 Å of thickness on each surface. This suggests that the protein adsorbs in a side-on conformation. Furthermore, as discussed previously, above certain protein coverage, no attractive force is observed as the surfaces are brought into contact. Measurements carried out after 29 h of protein adsorption in Figure 7 are similar to those obtained in Figure 6, where a protein concentration of 0.004 mg/mL was obtained by just one protein addition. This suggests that the system has reached equilibrium, with respect to adsorption at this concentration, as the force curves are independent of how the end concentration is reached.

Our reported data indicate protein multilayer adsorption in proteins with amphiphilic or flexible segments, as observed at

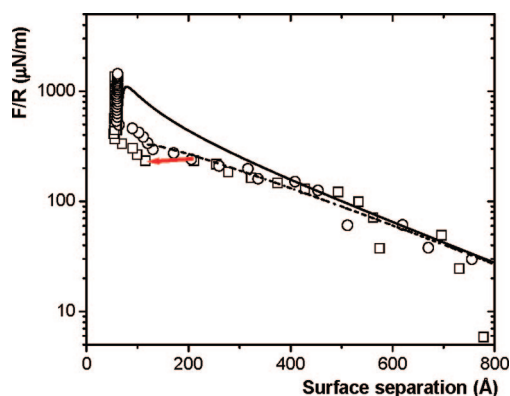


**Figure 6.** Force normalized by the radius of curvature,  $F/R$ , as a function of surface separation between mica surfaces adsorbed with Apo AII after 5 h ( $\square$ ) and 24 h ( $\circ$ ) of protein adsorption from a solution of 0.004 mg/mL. Lines indicate DLVO fitting with constant surface charge and dashed lines with constant surface potential. Details of the fittings can be found in the text. Arrows indicate attractive jumps.

SFA experiments with cytochrome  $c^{39}$  and  $\beta$ -casein.<sup>25</sup> A multilayer protein adsorption requires attractive protein–protein interaction, which often is weaker than the protein–surface interactions. This is illustrated in Figure 8, where it is shown the force recorded after replacing the protein solution (leaving a drop of protein solution between the mica surfaces separated  $\sim 2$  mm) with fresh acetic acid–sodium acetate buffer solution (pH = 4). The force curves recorded 1.5 and 18 h after dilution are shown together with the curve recorded just before exchanging the protein solution (29 h curve from Figure 7). The most significant change is that the hard wall separation has decreased from  $d \approx 58$  to  $d \approx 26$  Å and the apparent surface potential has increased from  $\sim 37$  to  $\sim 53$  mV 1.5 h after dilution, which indicates protein desorption. Even more protein has desorbed after 18 h, and the hard-wall separation reaches  $d \approx 11$  Å, corresponding to one monolayer on each surface. In addition, an attractive jump appears. No further desorption occurs, which is mostly likely due to the strong interaction between the negatively charged mica and the cationic protein as well as the entropy gain due to counterion release.

**Possible Biological Implications.** Our study could have biological implications where  $\alpha$ -helix amphiphilic membrane-binding motives are key variables. As an example, in antimicrobial peptides where available evidence suggests that linear peptides in solution fold into amphiphilic  $\alpha$ -helix upon binding the target membrane.<sup>40</sup> Also, in the case of the amphiphilic  $\alpha$ -helix apolipoproteins that tend to bind to the surface of lipoproteins. It is also

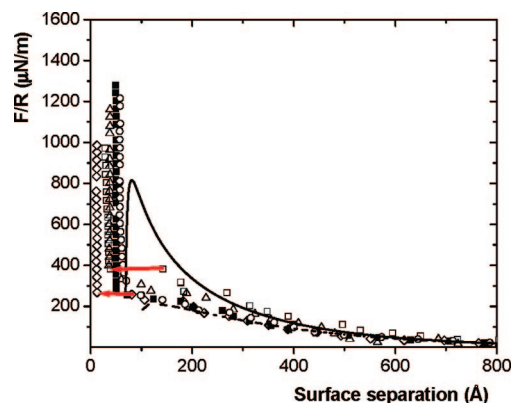


**Figure 7.** Force normalized by the radius of curvature,  $F/R$ , as a function of surface separation and total adsorption time between mica surfaces adsorbed with Apo AII. The total protein concentration was increased at two times during the experiment and it is: 0.002 mg/mL at 5 h ( $\diamond$ ), 0.004 mg/mL at 6.5 h ( $\square$ ), at 8 h ( $\Delta$ ), and 25 h ( $\blacksquare$ ), 29 h ( $\circ$ ). Lines indicate DLVO fitting (0.004 mg/mL) with constant surface charge and dashed lines with constant surface potential. Details of the fittings can be found in the text. Arrows indicate attractive jumps.

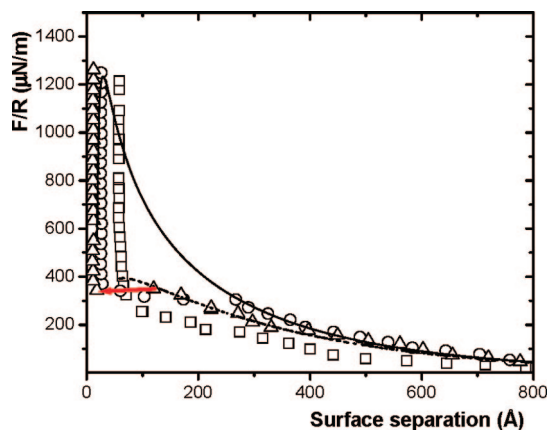


**Figure 8.** Force normalized by the radius of curvature,  $F/R$ , as a function of surface separation between mica surfaces adsorbed with Apo AII after protein dilution. Experiment after 29 h of adsorption time (protein concentration of 0.004 mg/mL) described in Figure 7 (□). Experiments for 1.5 (○) and 18 h (Δ) after protein dilution using a fresh protein-free acetic acid/sodium acetate buffer solution. In the latter curve, there is an attractive jump. Lines indicate DLVO fitting with constant surface charge and dashed lines with constant surface potential. Details of the fittings can be found in the text. Arrows indicate attractive jumps.

interesting to note that some lipoprotein-bound Apos are able to dissociate from the lipoprotein surface in a lipid-poor form, and then transferred through the plasma serum to other lipoproteins.<sup>41–45</sup> Although, this mechanism is poorly understood, it is known to be conducted by interactions between apolipoproteins located at the lipid surface. Hence our results could be of help to understand

(41) Castro, G. R.; Fielding, C. J. *J. Lipid Res.* **1984**, *25*, 58.

(42) Weinberg, R. B.; Spector, M. S. *J. Lipid Res.* **1985**, *26*, 26.

the interactions and involved molecular mechanisms in the apolipoprotein transfer.

#### 4. Conclusions

We have shown that the interaction forces between adsorbed Apo AII on the mica surfaces are mainly due to steric repulsive forces at small distances. At long distances, electrostatic double-layer is the most important contribution. Amphiphilicity of  $\alpha$ -helix structure facilitates the multilayer protein formation next to surfaces. At low protein coverage we found an attractive force related to different protein configurations at the adsorbed layers that could produce bridging or intercalating between the surfaces. Also, we have shown that the protein–surface interaction is stronger than protein–protein interaction. Apo AII is a double strand chain made of  $\alpha$ -helices with force interactions similar to those found in the single strand chain  $\alpha$ -helix Apo CI, suggesting that these force interactions are generic for this type of amphiphilic protein motif. Our results might have implications in understanding the way exchangeable apolipoproteins move in an aqueous environment between lipoproteins, as well as the way they associate and recognize target molecules at the cell membrane.

**Acknowledgment.** The support from CONACYT (36680-E and 47333-Q) and DGAPA-UNAM (IN110505 and 230303) is gratefully acknowledged. We also thank C. Garza for her technical support and S. Lindman for her help with CD measurements.

LA800348Y

(43) Liang, H. Q.; Rye, K. A.; Barter, P. J. *Biochim. Biophys. Acta* **1995**, *1257*, 31.

(44) Wang, G. *FEBS Lett.* **2002**, *529*, 157.

(45) Clay, M. A.; Cehic, D. A.; Pyle, D. U.; Rye, K. A.; Barter, P. J. *Biochem. J.* **1999**, *337*, 445.